International Journal of Heat and Mass Transfer 52 (2009) 3767–3777

Contents lists available at ScienceDirect

International Journal of Heat and Mass Transfer

journal homepage: www.elsevier.com/locate/ijhmt

One-dimensional model of evaporation and condensation in the presence of a noncondensable gas with applications to cryogenic fluid storage

Charles Panzarella [a], Mohammad Kassemi [b,*]

[a] Equity Engineering Group, 20600 Chagrin Blvd. Suite 1200, Shaker Heights, OH 44122, USA
[b] National Center for Space Exploration Research, NASA Glenn Research Center, 21000 Brookpark Rd., Mailstop 110-3, Cleveland, OH 44135, USA

ARTICLE INFO

Article history:
Received 11 July 2008
Received in revised form 19 February 2009
Accepted 19 February 2009
Available online 11 April 2009

Keywords:
Evaporation
Condensation
Noncondensable
Two-phase flow
Cryogenic storage
Zero boil off

ABSTRACT

This paper considers the one-dimensional flow of vapor between two liquid surfaces due to evaporation and condensation taking into account diffusion through a noncondensable gas and nonequilibrium interfacial kinetics. An explicit relationship is developed for the mass flux J as a function of the characteristic mole ratio of noncondensable gas X, and several simplifications are made to arrive at an effective heat transfer coefficient. A characteristic mole ratio X_c is also identified that demarcates the transition to a kinetically-limited regime when $X \ll X_c$ from a diffusively-limited regime when $X \gg X_c$. Numerical results obtained over a wide range of parameters show that even with a small amount of noncondensable gas, the interfacial temperature drop can be quite significant primarily because of diffusional resistance, an observation that has important practical implications, especially in the field of cryogenic fluid storage.

1. Introduction

Evaporation and condensation in the presence of a noncondensable gas is an important phenomenon with applications in several key technologies involving both ground-based and space-bound cryogenic storage tanks, phase separators and condensing heat exchangers [1]. There is a great deal of interest in knowing how the presence of a noncondensable gas affects the mass and heat transfer rates in such systems. This is of considerable importance to the design of space-based cryogenic storage tanks since these tanks are typically pressurized with helium to aid in the extraction of liquid propellant during engine startups. Under long-term storage conditions, variations in noncondensable concentrations could give rise to interfacial temperature gradients that are large enough to instigate surface-tension driven Marangoni convection. This effect could be favorably exploited in certain circumstances to provide a passive alternative to the inefficient forced mixing that is traditionally used to disrupt thermal stratification.

The effect of a noncondensable gas in the context of cryogenic fluid storage was studied very early on by Clark [1]. Solutions to one-dimensional heat conduction and mass diffusion equations were used to determine the interfacial temperature in the presence of a noncondensable gas. It was found that the condensation rate of oxygen was greatly reduced by the presence of the noncondensable gas helium. Subsequent work by Minkowycz and Sparrow [2] provided a much more comprehensive treatment of steam condensation onto an isothermal vertical plate with air as the noncondensable gas including the effects of superheating, free convection, mass diffusion, thermal diffusion and interfacial resistance. It was shown that even small amounts of noncondensable gas could significantly alter the heat transfer rate. This effect was shown to be almost entirely due to the diffusional resistance of the gas–vapor boundary layer at the interface. The interfacial resistance due to nonequilibrium kinetic effects was found to have a negligible effect.

More recent treatments can be broadly divided into those employing kinetic theory, irreversible thermodynamics or statistical rate theory to derive expressions for the interfacial mass and energy fluxes. Kinetic models of evaporation and condensation are based upon various approximate or numerical solutions of the Boltzmann kinetic equation. Schrage [3] obtains a relatively simple solution for pure vapor by assuming that its velocity distribution function takes the form of a perturbed Maxwellian with a single correction factor to account for the drift velocity of the evaporating or condensing vapor. The classical Hertz–Knudsen formulation does not account for this drift velocity since it is based solely upon equilibrium thermodynamics that assumes the bulk vapor is at rest. Labuntsov and Kryukov [4] developed a more sophisticated kinetic approach, although it is still limited to the case of pure vapor, by using a discontinuous, four-moment approximation to the velocity distribution function. Other studies [5–8] have extended

* Corresponding author. Tel.: +1 216 433 5031; fax: +1 216 433 5033.
E-mail address: Mohammad.Kassemi@nasa.gov (M. Kassemi).

0017-9310/$ - see front matter © 2009 Elsevier Ltd. All rights reserved.
doi:10.1016/j.ijheatmasstransfer.2009.02.027

Nomenclature

A	dimensionless parameter characterizing thermal boundary layer thickness, $A = J_{a0}c_{pv}d/k_m$
B	dimensionless parameter characterizing steepness of saturation pressure relationship, $B = Lm_v/RT_{l0}$
c_p	specific heat at constant pressure
d	distance between evaporating and condensing interfaces
D	mass diffusion coefficient
D^T	thermal diffusion coefficient
E	energy flux
h	enthalpy
J	mass flux
J'	dimensionless mass flux, $J' = J/J_{a0}$
J_a	absolute (maximum) rate of evaporation
J'_{min}	minimum diffusive mass flux, $J'_{min} = X_c\Delta p'_s$
k	thermal conductivity
L	latent heat of vaporization
m	molecular weight
p	pressure
$\bar{p}$	average pressure or mean of boundary pressures
p'	dimensionless pressure, $p' = p/p_{s0}$
Δp	pressure drop between evaporating and condensing interfaces, $\Delta p = p_0 - p_d$
$\tilde{p}_{g0}$	approximate noncondensable gas pressure at evaporating interface, $\tilde{p}_{g0} = \bar{\rho}_g RT_{l0}/m_g$
q	heat flux
q_{min}	minimum heat flux required to sustain specified liquid temperature drop, $q_{min} = (\kappa + k_m)\Delta T_l/d$
R	ideal gas constant
T	temperature
T'	dimensionless temperature, $T' = T/T_{l0}$
$\bar{T}$	average temperature
ΔT	temperature drop between evaporating and condensing interfaces, $\Delta T = T_0 - T_d$
X	approximate mole ratio of noncondensable gas to vapor, $X = \tilde{p}_{g0}/p_{s0} = \bar{\rho}_g RT_{l0}/m_g p_{s0}$
X_c	critical mole ratio for determining the relative importance of diffusive and kinetic effects, $X_c = m_v D_m p_{s0}/RdJ_{a0}T_{l0}$
z	distance from evaporating interface
z'	dimensionless distance, $z' = z/d$

Greek Symbols

α	accommodation coefficient
α_T	thermal diffusion factor
κ	effective thermal conductivity due to mass transfer, $\kappa = L^2 m_v^2 D_m p_{s0}/R^2 T_{l0}^3$
ω	vapor mass fraction
ρ	mass density
$\bar{\rho}$	average mass density

Subscripts

0	pertaining to evaporating interface at $z = 0$
b	normal boiling point
c	critical
d	pertaining to condensing interface at $z = d$
g	noncondensable gas
l	liquid
m	vapor–gas mixture
r	reference
s	saturation
v	vapor

this approach to account for noncondensable gas effects and have shown that even a trace amount of noncondensable gas can have a significant effect on the condensation rate.

The methods of irreversible thermodynamics have also been used [9–11] to derive alternative expressions for the interfacial fluxes that involve a number of undetermined phenomenological coefficients, which can be estimated from kinetic theory [12,13], molecular dynamics simulations [14] or by comparison with experimental measurements [11]. This approach has generally shown good agreement with experimental measurements if the coefficients are chosen properly [15,16].

The recent evaporation and condensation experiments of Fang and Ward [17,18] and Ward and Stanga [19] show larger temperature jumps across the interface than previously expected (up to 7.8 K in some cases). In order to explain these results, they have proposed an alternative approach known as statistical rate theory (SRT) that is based upon the quantum mechanical concept of transitional probability [20]. However, as pointed out by Bond and Struchtrup [15,16], although SRT does provide good predictive ability for the mass flux, it is still an incomplete theory because it does not yet provide an expression for the interfacial heat flux required for a complete solution. They also show that the linearized SRT mass flux is equivalent to the mass flux expression provided by irreversible thermodynamics. They conclude that since SRT and irreversible thermodynamics yield essentially the same results, the nonlinear SRT expression does not provide any significant additional predictive capability.

Bond [15] also shows that all three approaches (kinetic theory, irreversible thermodynamics and SRT) predict mass fluxes that agree with experimental measurements [17–19] as long as the phenomenological coefficients are chosen appropriately. The irreversible thermodynamics energy flux also closely predicts the interfacial temperature jump and direction. The kinetic model of Schrage [3] is unable to predict the correct temperature jump unless it is augmented by a velocity-dependent condensation coefficient.

The current paper is concerned with the flow of vapor between two flat liquid surfaces held at different temperatures with noncondensable gas in the intervening vapor region. Our approach is based upon the original analysis of Plesset [21] except that we also include the effects of vapor diffusion through a noncondensable gas, and we have selected the kinetic theory of Schrage [3] to account for nonequilibrium interfacial effects instead of the Hertz–Knudsen relation. Since this paper mainly focuses on the diffusive effects of the noncondensable gas, the Schrage [3] model was deemed to be suitable for now. Future work will incorporate a more comprehensive kinetic model such as Pong and Moses [5] that does directly take into account noncondensable gas effects. The bulk vapor region is treated from a continuum point of view and kinetic effects are included only by modifying the interfacial boundary conditions. One-dimensional balances of energy and mass result in several useful relationships between the rate of mass transfer, the mole fraction of noncondensable gas, and the imposed interfacial temperature drop. Simplified engineering correlations are obtained by considering various limiting cases. Our analysis also determines when a transition from a diffusion-limited regime to a kinetically-limited regime will occur by identifying a critical mole ratio of noncondensable gas. Numerical results are presented for case studies typically encountered in the area of space-based and ground-based cryogenic storage of propellant or life-support fluids.

2. Mathematical model

Consider two flat liquid–vapor interfaces at different temperatures separated by a distance d with a mixture of vapor and noncondensable gas in the intervening gap as shown in Fig. 1. The interfacial temperature difference drives a flow of vapor between the evaporating interface at $z = 0$ and the condensing interface at $z = d$, where z is the perpendicular distance from the evaporating interface. By enforcing mass and energy balances through the vapor gap while taking into account the diffusion of vapor through the noncondensable gas, it is possible to derive a simple implicit relationship for the vapor mass flux J as a function of the imposed liquid temperature drop.

For the sake of generality, it is important to distinguish between the temperature on the liquid and vapor sides of each interface since they can, in general, be different when kinetic effects become important. For the evaporating interface at $z = 0$, let T_{l0} and T_{v0} be the temperatures on the liquid and vapor side, respectively. Likewise, let T_{ld} and T_{vd} be the respective liquid and vapor temperatures for the condensing interface at $z = d$. Let p_{v0} and p_{vd} denote the interfacial vapor pressures and p_{s0} and p_{sd} the equilibrium saturation pressures corresponding to T_{l0} and T_{ld}, respectively.

2.1. Properties of the vapor–gas mixture

Assuming ideal gas behavior, the total pressure p_m at any point within the vapor–gas mixture is given by the sum of the vapor and gas partial pressures,

$$p_m = p_v + p_g, \tag{1}$$

where p_v is the partial vapor pressure and p_g is the partial pressure of the noncondensable gas. Let the average total pressure $\bar{p}$ be defined by $\bar{p} = d^{-1}\int_0^d p_m\,dz$. For the problem at hand, it is assumed that the hydrostatic, inertial and viscous pressure scales are many orders of magnitude less than the total pressure, $|(p_m - \bar{p})/\bar{p}| \ll 1$, so that the total pressure can simply be regarded as a constant equal to its average value, i.e. $p_m \approx \bar{p}$. Plesset [21] also showed that this assumption is valid as long as the flow velocity is much less than the speed of sound.

The vapor and noncondensable gas each satisfy a separate equation of state at the common temperature T_v (the temperature of the vapor and noncondensable gas are assumed to be equal),

$$\rho_v = \frac{m_v p_v}{RT_v}, \tag{2}$$

$$\rho_g = \frac{m_g p_g}{RT_v}, \tag{3}$$

where m_v and m_g are the molar masses of the vapor and gas molecules, respectively, and R is the ideal gas constant. A combined equation of state in terms of these densities can be obtained by substituting Eqs. (2) and (3) into Eq. (1) assuming $p_m \approx \bar{p}$,

$$\frac{\bar{p}}{RT_v} = \frac{\rho_v}{m_v} + \frac{\rho_g}{m_g}. \tag{4}$$

If we define the total mixture density ρ_m by

$$\rho_m = \rho_v + \rho_g, \tag{5}$$

then we can define the vapor mass fraction ω by,

$$\omega = \frac{\rho_v}{\rho_m}. \tag{6}$$

By rearranging Eq. (6), we get,

$$\rho_v = \rho_m \omega, \tag{7}$$

and by substituting this back into Eq. (5) and solving for ρ_g, we see that,

$$\rho_g = \rho_m(1-\omega). \tag{8}$$

Substituting Eqs. (7) and (8) into Eq. (4) and solving for ρ_m results in a useful expression relating the total density to the average pressure and vapor mass fraction,

$$\rho_m = \frac{\bar{p}}{RT_v}\frac{m_v m_g}{(1-\omega)m_v + \omega m_g}. \tag{9}$$

Finally, substitution of Eq. (7) into Eq. (2) with ρ_m given by Eq. (9) results in,

$$p_v = \frac{m_g \omega}{m_v(1-\omega) + m_g\omega}\bar{p}. \tag{10}$$

Since $p_g = \bar{p} - p_v$, the partial pressure of the noncondensable gas can be written similarly as,

$$p_g = \frac{m_v(1-\omega)}{m_v(1-\omega) + m_g\omega}\bar{p}. \tag{11}$$

2.2. Equations governing mass and energy transfer through the vapor–gas mixture

The vapor mass flux moving through the gap is defined by $J = \rho_v u_v$, where u_v is the average velocity of the vapor molecules with respect to either interface. If we define the mass-averaged velocity u_m by $u_m = \omega u_v + (1-\omega)u_g$, where u_g is the average velocity of the gas molecules, then J can be decomposed into two contributions as follows, $J = \rho_v u_m + \rho_v(u_v - u_m)$. The first term is a convective contribution, and the second term is the diffusive mass flux which, in general, is proportional to gradients of the mass fraction, pressure and temperature. Since the total pressure is constant, only gradients of mass fraction and temperature will play any role, so we can write the diffusive term as $\rho_v(u_v - u_m) = -\rho_m D_m \mathrm{d}\omega/\mathrm{d}z - D^T \mathrm{d}(\ln T)/\mathrm{d}z$, where D_m is the mass diffusion coefficient for the vapor–gas mixture and D^T is the thermal diffusion coefficient. According to Bird [22], the ratio $D^T/\rho_m D_m$ can be written as $D^T/\rho_m D_m = \alpha_T\omega(1-\omega)$, where α_T is the thermal diffusion factor, which experimental measurements have shown is nearly independent of concentration for gas mixtures. Also, since the gas is stagnant at steady state ($u_g = 0$), we get $u_m = \omega u_v$ so that the convective term becomes $\rho_v u_m = \rho_v \omega u_v = \omega J$. By combining all of these relationships, the expression for J becomes,

$$J = -\rho_m D_m\left(\frac{1}{1-\omega}\frac{\mathrm{d}\omega}{\mathrm{d}z} + \alpha_T\frac{\omega}{T}\frac{\mathrm{d}T}{\mathrm{d}z}\right). \tag{12}$$

Before going any further, however, the second term in this equation, which is due to Soret (thermal) diffusion, will be neglected. This is justified for two reasons. First, the value of the thermal diffusion

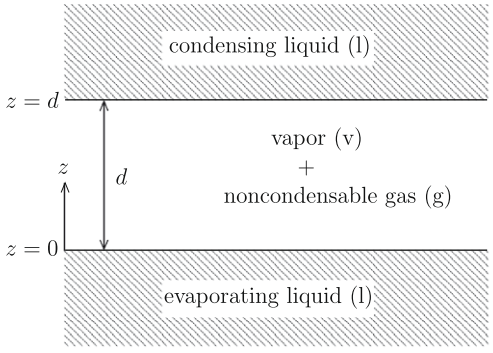

Fig. 1. The one-dimensional model used here to study mass transfer between an evaporating and condensing interface with some noncondensable gas in between.

factor α_T is normally small for the gas mixtures of interest here. For example, according to Hirschfelder [23], $\alpha_T = 0.14$ for a $He - H_2$ mixture at 46 K. Additionally, in the next section a small temperature drop assumption will be invoked. The combined effect of these two considerations will make the exclusion of the thermal diffusion term justified in the context of this paper. In future work that does not invoke the small temperature drop assumption, the Soret term will be retained throughout the analysis to assess and characterize its effects, especially in the thermal boundary layer that may develop near the condensing interface at high evaporation (advective mass transfer) rates.

By neglecting the thermal diffusion term, the mass flux expression simplifies to,

$$J = -\frac{\rho_m D_m}{1-\omega}\frac{d\omega}{dz}. \tag{13}$$

Since J must be constant throughout the gap at steady state, the solution for ω can be obtained by solving the equation $dJ/dz = 0$ after first substituting Eq. (9) for ρ_m into Eq. (13), assuming D_m and $\bar{p}$ are constant. Once the solution for ω is known, it can be substituted back into Eq. (13), which can then be converted into an expression in terms of partial pressure instead of ω by making use of Eq. (10) to arrive at the final expression for the mass flux,

$$J = \frac{\bar{p} m_v D_m}{R \bar{T}_v d} \ln\left(\frac{\bar{p} - p_{vd}}{\bar{p} - p_{v0}}\right), \tag{14}$$

where $\bar{T}_v$ is the average vapor temperature defined by $\bar{T}_v \equiv d^{-1}\int_0^d T_v dz$.

The vapor temperature T_v can be found by requiring that the net energy flux E through the gap, consisting of both conductive and convective contributions (but neglecting compressible work and the Dufour effect), be constant at steady state. Assuming the vapor enthalpy h_v has the ideal-gas form $h_v = c_{pv}(T_v - T_{v0}) + h_{v0}$, where c_{pv} and h_{v0} are constants, this can be represented as

$$\frac{dE}{dz} = \frac{d}{dz}\left(-k_m\frac{dT_v}{dz} + Jc_{pv}(T_v - T_{v0})\right) = 0, \tag{15}$$

where k_m is the mixture thermal conductivity. Since J is constant at steady state, this equation can be readily integrated across the vapor gap subject to the boundary conditions $T_v = T_{v0}$ at $z = 0$ and $T_v = T_{vd}$ at $z = d$ (assuming constant k_m) to yield the desired vapor temperature solution,

$$\frac{T_{v0} - T_v}{\Delta T_v} = \frac{1 - \exp[(Jc_{pv}/k_m)z]}{1 - \exp[(Jc_{pv}/k_m)d]}, \tag{16}$$

where $\Delta T_v = T_{v0} - T_{vd}$. This equation can be readily integrated to obtained the average vapor temperature $\bar{T}_v$ required in Eq. (14).

The average total pressure $\bar{p}$ appearing in Eq. (14) can be found by integrating Eq. (3) across the vapor gap from $z = 0$ to $z = d$, resulting in the following constraint on $\bar{p}$,

$$\bar{\rho}_g = \frac{m_g(\bar{p} - p_{v0})}{Rd}\int_0^d \frac{1}{T_v}\left(\frac{\bar{p} - p_{v0}}{\bar{p} - p_{vd}}\right)^{-\int_0^z (T_v/\bar{T}_v d)\,dz} dz. \tag{17}$$

Thus, given the average gas density $\bar{\rho}_g$, which is assumed to be a known quantity, the total pressure $\bar{p}$ can be found by satisfying Eq. (17).

2.3. Kinetic boundary conditions at the interface

The link between the liquid and vapor interfacial temperatures is provided by using an appropriate kinetic model of phase change. Despite the plethora of kinetic models to choose from, it was decided to use the simple but comprehensive kinetic model first presented by Schrage [3], which assumes the vapor velocity distribution takes the form of a perturbed Maxwellian distribution and then uses balances of mass, momentum and energy across the Knudsen layer to determine the extent of the temperature and pressure jumps across this layer in addition to determining the magnitude of the interfacial mass flux. The relationships provided by this model are a little unwieldy in their original form because they are written implicitly in parametric form. A more convenient form is obtained in Panzarella [24] by simply rewriting them as explicit functions of the interfacial mass flux as follows,

$$\frac{p_v}{p_s} = \frac{3}{4\pi}\left(\frac{\pi}{2} - \frac{J}{J_a}\right) + \frac{5}{4\pi}\sqrt{\left(\frac{\pi}{2} - \frac{J}{J_a}\right)^2 - \frac{2\pi}{5}\frac{J^2}{J_a^2}}, \tag{18}$$

$$\frac{T_v}{T_l} = \left[\frac{4}{5} + \frac{1}{5}\frac{p_s}{p_v}\left(1 - \frac{2}{\pi}\frac{J}{J_a}\right)\right]^{-1}, \tag{19}$$

where p_s is the equilibrium saturation pressure dependent upon the liquid temperature and J_a is the absolute rate of evaporation defined by,

$$J_a(T) = \alpha p_s\sqrt{\frac{m_v}{2\pi RT}}, \tag{20}$$

where α is the accommodation coefficient (fraction of incident vapor molecules that enter the liquid phase). An explicit expression for the saturation pressure is given by the Clausius–Clapeyron equation for an ideal gas,

$$p_s(T_l) = p_r \exp\left[\frac{Lm_v}{R}\left(\frac{1}{T_r} - \frac{1}{T_l}\right)\right], \tag{21}$$

where T_r is the known saturation temperature at some reference pressure p_r and L is the latent heat of vaporization.

2.4. Dimensionless equations

If two liquid interfaces are separated by a distance d and maintained at the different temperatures T_{l0} and T_{ld}, then the resulting vapor mass flux J between them due to evaporation at one interface and condensation at the other can be determined by simultaneously solving for the two unknowns J and $\bar{p}$ from the implicit relationships given by Eqs. (14) and (17). Additional relationships between the liquid and vapor interfacial temperatures and pressures are provided by Eqs. (18) and (19), which are derived from a particular nonequilibrium kinetic theory. It should be noted that this model could be extended very easily to make use of any other nonequilibrium interfacial condition by simply replacing Eqs. (18) and (19) by whatever relationships for the pressure and temperature discontinuities that would be provided by the alternative treatment.

These equations can be written in dimensionless form by defining the scaled variables $J' = J/J_{a0}$ and $\bar{p}' = \bar{p}/p_{s0}$, where $J_{a0} = J_a(T_{l0})$. Then, Eqs. (14) and (17) become,

$$J' = \frac{\bar{p}'}{\bar{T}'_v} X_c \ln\left(\frac{\bar{p}' - p'_{vd}}{\bar{p}' - p'_{v0}}\right), \tag{22}$$

$$X = (\bar{p}' - p'_{v0})\int_0^1 \frac{1}{T'_v}\left(\frac{\bar{p}' - p'_{v0}}{\bar{p}' - p'_{vd}}\right)^{-\int_0^{z'} (T'_v/\bar{T}'_v)\,dz'} dz'. \tag{23}$$

Here, $X = \bar{\rho}_g RT_{l0}/m_g p_{s0}$ is the characteristic mole ratio of noncondensable gas and $X_c = m_v D_m p_{s0}/RdJ_{a0}T_{l0}$ is a critical mole fraction. The significance of these parameters and the reason for this naming convention will become clear later on. Finally, $z' = z/d$ is the dimensionless distance from the evaporating interface ($0 \leqslant z' \leqslant 1$).

Similarly, the scaled vapor temperature $T'_v = T_v/T_{l0}$ and its average value $\bar{T}'_v = \bar{T}_v/T_{l0}$ satisfy the following dimensionless equations,

$$T'_v(z') = T'_{v0} - \Delta T'_v \frac{1 - e^{AJ'z'}}{1 - e^{AJ'}}, \tag{24}$$

$$\bar{T}'_v = T'_{v0} - \Delta T'_v \left(\frac{1}{1 - e^{AJ'}} + \frac{1}{AJ'} \right), \tag{25}$$

$$\int_0^{z'} T'_v dz' = T'_{v0} z' - \Delta T'_v \left(\frac{AJ'z' + 1 - e^{AJ'z'}}{AJ'(1 - e^{AJ'})} \right), \tag{26}$$

where $\Delta T'_v = T'_{v0} - T'_{vd}$, and $A = J_{a0} c_{pv} d / k_m$ is another dimensionless parameter. The boundary vapor temperatures are defined by $T'_{v0} = T_{v0}/T_{l0}$ and $T'_{vd} = T_{vd}/T_{l0} = (T_{vd}/T_{ld})T'_{ld}$, where $T'_{ld} = T_{ld}/T_{l0}$. Unlike the liquid boundary temperatures, these are not constant but functions of the mass flux rate J' according to the dimensionless version of Eq. (19),

$$T'_{v0} = \left[\frac{4}{5} + \frac{1}{5p'_{v0}} \left(1 - \frac{2}{\pi} J' \right) \right]^{-1}, \tag{27}$$

$$T'_{vd} = T'_{ld} \left[\frac{4}{5} + \frac{p'_{sd}}{5p'_{vd}} \left(1 + \frac{2}{\pi} \frac{J'}{J'_{ad}} \right) \right]^{-1}, \tag{28}$$

where $J'_{ad} = J_{ad}/J_{a0}$ and $p'_{sd} = p_{sd}/p_{s0}$ are given by,

$$J'_{ad} = \frac{J_{ad}}{J_{a0}} = \frac{p'_{sd}}{\sqrt{T'_{ld}}}, \tag{29}$$

$$p'_{sd} = \exp\left[B \left(1 - \frac{1}{T'_{ld}} \right) \right], \tag{30}$$

with $J_{ad} = J_a(T_{ld})$ and $B = Lm_v/RT_{l0}$. The sign of J' is reversed in Eq. (28) because mass is condensing at that interface.

Finally, the dimensionless boundary vapor pressures are defined by $p'_v = p_{v0}/p_{s0}$ and $p'_{vd} = p_{vd}/p_{s0} = (p_{vd}/p_{sd})p'_{sd}$. They also depend on J' according to dimensionless versions of Eq. (18),

$$p'_{v0} = \frac{3}{4\pi} \left(\frac{\pi}{2} - J' \right) + \frac{5}{4\pi} \sqrt{ \left(\frac{\pi}{2} - J' \right)^2 - \frac{2\pi}{5} J'^2 }, \tag{31}$$

$$p'_{vd} = p'_{sd} \left[\frac{3}{4\pi} \left(\frac{\pi}{2} + \frac{J'}{J'_{ad}} \right) + \frac{5}{4\pi} \sqrt{ \left(\frac{\pi}{2} + \frac{J'}{J'_{ad}} \right)^2 - \frac{2\pi}{5} \frac{J'^2}{J'^2_{ad}} } \right]. \tag{32}$$

Again, the sign of J' is reversed in Eq. (32) because mass is condensing at that interface.

Thus, the one-dimensional solution for the dimensionless mass flux J' depends in the most general case on exactly five dimensionless parameters, $J' = J'(T'_{ld}, X, X_c, B, A)$. The parameter X deserves special attention since it is a direct measure of the amount of noncondensable gas present. Even though the partial pressure of the noncondensable gas varies from point to point within the vapor gap, the quantity defined by $\tilde{p}_{g0} = \bar{\rho}_g RT_{l0}/m_g$ is a constant that is characteristic of this pressure. Indeed, $\tilde{p}_{g0}$ can be regarded as the pressure that would be exerted by the noncondensable gas on the evaporating interface if its density at that location were equal to the average gas density $\bar{\rho}_g$. With this in mind, the parameter X can be written more compactly as $X = \tilde{p}_{g0}/p_{s0}$, and then it should be evident why X is referred to as the "characteristic mole ratio" of noncondensable gas with respect to the vapor.

3. Solution for small temperature drop

The dimensionless liquid temperature drop is defined by $\Delta T'_l = (T_{l0} - T_{ld})/T_{l0} = 1 - T'_{ld}$. When $|\Delta T'_l| \ll 1$, it follows that the vapor temperature drop is also small, i.e. $|\Delta T'_v| \ll 1$. When $|\Delta T'_v| \ll 1$, then to leading order, the terms proportional to $\Delta T'_v$ in Eqs. (24) and (25) can be neglected with respect to the dominant term T'_{v0} for any value of A or J'. Then, both T'_v and its average value $\bar{T}'_v$ can be replaced by T'_{v0} in Eq. (23). It is then possible to show that Eqs. (22) and (23) simplify considerably and can be combined into the single equation,

$$J' = \frac{X_c}{X} \left[\bar{p}'_v + \frac{\Delta p'_v}{2} \coth\left(\frac{\Delta p'_v}{2XT'_{v0}} \right) \right] \frac{\Delta p'_v}{T'^2_{v0}}. \tag{33}$$

This is the small temperature drop approximation that will be used throughout the remainder of this paper. The only assumption required to arrive at Eq. (33) is that $|\Delta T'_l| \ll 1$. No restriction on J' or any other parameter was involved. Thus, Eq. (33) is valid over the entire range of mass flux from the kinetically-limited regime all the way up to the diffusion-limited regime.

3.1. Diffusion-limited regime

If $|J'| \ll 1$ (evaporative mass flux much less that its absolute kinetic limit), then we can assume that the liquid and vapor interfacial temperatures are equal ($T'_{v0} = 1, T'_{vd} = T'_{ld}$) and that the vapor boundary pressures can be replaced by the corresponding saturation pressures ($p'_{v0} = 1$ and $p'_{vd} = p'_{sd}$). This also follows from setting $J' = 0$ in Eqs. (27), (28), (31) and (32). Then, if we define $\bar{p}'_s = (p_{s0} + p_{sd})/2p_{s0} = (1 + p'_{sd})/2$ and $\Delta p'_s = (p_{s0} - p_{sd})/p_{s0} = 1 - p'_{sd}$, Eq. (33) reduces to an explicit expression for J' in terms of known parameters,

$$J' = \frac{X_c}{X} \left[\bar{p}'_s + \frac{\Delta p'_s}{2} \coth\left(\frac{\Delta p'_s}{2X} \right) \right] \Delta p'_s. \tag{34}$$

Since J' increases as $X \to 0$, Eq. (34) is strictly valid only as long as X does not get so small that the assumption $|J'| \ll 1$ is violated. When $X \ll |\Delta p'_s|/2, \coth(\Delta p'_s/2X) \approx 1$ and Eq. (34) has the limiting behavior,

$$J' \approx \frac{X_c}{X} \left[\bar{p}'_s + \frac{|\Delta p'_s|}{2} \right] \Delta p'_s. \tag{35}$$

In order to satisfy the condition $J' \ll 1$, the mole ratio must satisfy the restriction,

$$\frac{X}{X_c} \gg \left[\bar{p}'_s + \frac{|\Delta p'_s|}{2} \right] \Delta p'_s. \tag{36}$$

As long as this condition is satisfied, then we are in a diffusion-limited regime, and it is appropriate to use Eq. (34) to predict the mass flux. Since $\bar{p}'_s \approx 1$ and $\Delta p'_s \leqslant 1$, Eq. (36) is satisfied as long as $X \gg X_c$. As will be shown later, for typical parameter values of hydrogen at its normal boiling point, $X_c \approx 10^{-6}$, so Eq. (34) is valid for most practical situations where the amount of noncondensable gas is not vanishingly small.

In the opposite extreme when $X \gg |\Delta p'_s|/2, J'$ approaches the constant value J'_{min},

$$J' \approx J'_{min} = X_c \Delta p'_s. \tag{37}$$

In this limit, the vapor pressure is negligible when compared to the noncondensable gas pressure. Again, Eq. (37) is only valid as long as $|J'| = |X_c \Delta p'_s| \ll 1$. Because of the vanishingly small value of X_c, this condition is also automatically satisfied under most normal conditions. Therefore, Eq. (34) can be rewritten as,

$$\frac{J'}{J'_{min}} = \frac{1}{X} \left[\bar{p}'_s + \frac{\Delta p'_s}{2} \coth\left(\frac{\Delta p'_s}{2X} \right) \right], \tag{38}$$

which is independent of the parameter X_c and, thus, depends on the noncondensable gas only through the mole ratio X. Eq. (38) is valid as long as $X \gg X_c$ so that $|J'| \ll 1$.

A uniformly-valid approximation to Eq. (38) that has the correct limiting behavior given by Eq. (35) when $X \ll \Delta p'_s/2$ and Eq. (37) when $X \gg \Delta p'_s/2$ is,

$$\frac{J'}{J'_{min}} = \frac{\bar{p}'_s + |\Delta p'_s|/2}{X} + 1. \tag{39}$$

The error of this approximation is greatest when $X \approx \Delta p'_s/2$, but it is relatively small when $|\Delta p'_s| \ll 1$ and goes to zero as $|\Delta p'_s| \to 0$.

Note that the dimensionless saturation pressure condition given by Eq. (30) can be written in terms of $\Delta T'_l$ as,

$$p'_{sd} = \exp\left(\frac{-B\Delta T'_l}{1-\Delta T'_l}\right). \tag{40}$$

Thus, if we assume that $|B\Delta T'_l| \ll 1$ in addition to $|\Delta T'_l| \ll 1$, then Eq. (40) can be approximated by its first two terms in a Taylor series expansion,

$$p'_{sd} = 1 - B\Delta T'_l, \tag{41}$$

and then $\Delta p'_s = 1 - p'_{sd} = B\Delta T'_l$ and $\bar{p}'_s = 1$. Eq. (39) would then simplify even further to,

$$\frac{J'}{J'_{min}} = \frac{1}{X} + 1, \tag{42}$$

and Eq. (37) becomes $J'_{min} = X_c B\Delta T'_l$. Eq. (42) is very good approximation to Eq. (38) for any mass fraction X as long as $|\Delta p'_s| \ll 1$. It could alternatively be written in terms of $\Delta T'_l$ directly as,

$$J' = \left(\frac{1}{X} + 1\right) X_c B\Delta T'_l. \tag{43}$$

3.2. Kinetically-limited regime

In the limit as $X \to 0$ (pure vapor with no noncondensable gas), we must have $\Delta p'_v = O(X)$ in Eq. (33) in order for J' to remain bounded and non-zero. Thus, the term proportional to $\Delta p'_v$ in the square brackets of Eq. (33) is negligible with respect to the other term, and we get the following simpler relationship,

$$\frac{X}{X_c} J' = \frac{\bar{p}'_v}{T'^2_{v0}} \Delta p'_v. \tag{44}$$

Since we are now in a kinetically-limited regime, J' is no longer negligible in Eqs. (31) and (32) and we cannot ignore the terms involving J'. However, instead of using the most general relationships, we will only use their linear approximations given by,

$$p'_{v0} = 1 - \frac{2}{\pi} J', \tag{45}$$

$$p'_{vd} = p'_{sd} + \frac{2}{\pi} J', \tag{46}$$

where we have assumed Eq. (29) reduces to $J'_{ad} = p'_{sd}$ since $T'_{ld} \approx 1$ when the small temperature drop approximation is invoked. Eqs. (45) and (46) are strictly only valid when $|J'| \ll 1$, however, it is a reasonable approximation even for evaporation rates (positive J) up to the absolute limit. Since the rate of condensation must always be equal to $-J$ in this one-dimensional problem, the linear approximation remains a good one even at the condensing interface.

By adding and subtracting Eqs. (45) and (46), we can write,

$$\Delta p'_v = \Delta p'_s - \frac{4}{\pi} J', \tag{47}$$

$$\bar{p}'_v = \bar{p}'_s. \tag{48}$$

Through substitution of Eqs. (47) and (48) into Eq. (44) and assuming $T'_{v0} = 1$ (from the small temperature drop approximation), Eq. (44) can be solved for J' with the result,

$$J' = \frac{\pi}{4} \Delta p'_s \left(1 + \frac{\pi}{4} \frac{X}{\bar{p}'_s X_c}\right)^{-1}. \tag{49}$$

Note that in the pure vapor limit when $X = 0$, the mass flux approaches a constant value given by,

$$J' = \frac{\pi}{4} \Delta p'_s. \tag{50}$$

This could also be obtained directly from Eq. (47) by setting $\Delta p'_v = 0$, which is consistent with the pure-vapor, kinetic limit already discussed previously at the end of Section 2.2.

3.3. Uniformly-valid approximation

We have seen that Eq. (34) is a good approximation to Eq. (33) when $X/X_c \gg 1$ and that Eq. (49) is a good approximation when $X/X_c \ll 1$ and $X \ll |\Delta p'_s|$. However, as long as $|\Delta p'_s| \ll 1$, Eqs. (35) and (49) are identical and there is an overlap region $X_c \ll X \ll |\Delta p'_s|$ where both approximations are equally valid. Therefore, we can construct a uniformly-valid approximation to Eq. (33) that determines J explicitly over the entire range of X/X_c by merging Eqs. (34) and (49) into this single, semi-heuristic equation,

$$\frac{J'}{J'_{min}} = \frac{1}{X + 4X_c(\bar{p}'_s + |\Delta p'_s|/2)/\pi} \left[\bar{p}'_s + \frac{\Delta p'_s}{2} \coth\left(\frac{\Delta p'_s}{2X}\right)\right]. \tag{51}$$

Note that Eq. (51) has the correct (very close) limiting behavior when $X/X_c \ll 1$ and $X/X_c \gg 1$. We should also note that Eq. (51) places no restriction on $|\Delta p'_s|$ when $X/X_c \gg 1$ since the mass flux is diffusion-limited in that case. Eq. (51) can be further simplified through the use of Eq. (39) to yield a good approximation for any X,

$$\frac{J'}{J'_{min}} = \frac{\bar{p}'_s + |\Delta p'_s|/2}{X + 4X_c(\bar{p}'_s + |\Delta p'_s|/2)/\pi} + 1. \tag{52}$$

The error of this approximation is greatest when $X \approx |\Delta p'_s|/2$, but the relative error is small when $|\Delta p'_s| \ll 1$ and goes to zero as $|\Delta p'_s| \to 0$.

4. Numerical results

In order to better illustrate the behavior of the evaporating/condensing system depicted in Fig. 1, a particular numerical example is given here for liquid hydrogen pressurized by the noncondensable gas helium. Numerical solutions demonstrating the behavior of this system will now be generated using the most general form of the implicit small-temperature drop relationship given by Eq. (33) and compared to the predictions of the explicit uniform approximation given by Eq. (52). In order to accomplish this, estimated values of the dimensionless parameters X_c and B are required. If we assume the operating conditions are close to the normal boiling point of hydrogen, then $T_{l0} = T_b = 20.39$ K, and we obtain values for the properties $p_{s0} = p_b, L, m_v$ and R from Table 1. An estimate of the absolute rate of evaporation, $J_{a0} = 13.94$ g/cm^2 s, is also obtained from Eq. (20) assuming $\alpha = 1$.

The mass diffusion coefficient D_m can be estimated from an empirical formula for a binary mixture of gases at low to moderate pressures given in Bird, Stewart and Lightfoot [22],

$$\frac{pD_m}{(p_{cv}p_{cg})^{1/3}(T_{cv}T_{cg})^{5/12}(1/m_v + 1/m_g)^{1/2}} = a\left(\frac{T}{\sqrt{T_{cv}T_{cg}}}\right)^b, \tag{53}$$

where p_{cv}, p_{cg} and T_{cv}, T_{cg} are the critical pressures and temperatures of the vapor and gas (in units of atm) and $a = 2.745 \times 10^{-4}$ and $b = 1.823$ are empirically-determined constants. When the noncondensable gas is helium, $m_g = 4.003$ g/mol, $T_{cg} = 5.195$ K and $p_{cg} = 2.244$ atm and from Eq. (53) we find that $D_m = 0.0139$ cm^2/s for this mixture at the normal boiling point temperature $T = 20.39$ K of hydrogen.

Table 1
Material properties of saturated hydrogen at its normal boiling point [25].

c_{pl}/erg (gK)$^{-1}$	9.74×10^7	c_{pv}/erg (gK)$^{-1}$	1.23×10^8
k_l/erg (cm s K)$^{-1}$	10356	k_v/erg (cm s K)$^{-1}$	1714
L/erg s^{-1}	4.45×10^9	m_v/g mol^{-1}	2.016
p_b/atm	1.0	R/erg (K mol)$^{-1}$	8.31×10^7
ρ_l/g cm^{-3}	0.070668	ρ_v/g cm^{-3}	0.0013801
T_b/K	20.39	T_c/K	33.19
p_c/atm	12.98		

Using these property values and assuming an interfacial spacing of $d = 1$ cm, the dimensionless parameters take the values of $X_c = 1.20 \times 10^{-6}$ and $B = 5.3$. Consequently, the values $X_c = 10^{-6}$ and $B = 5$ are used here to generate the baseline solutions to Eqs. (33) and (52). The results are shown in Fig. 2a over a wide range of mole ratio X for three different values of $\Delta T_l'$. First, note the very good agreement between the exact and approximate solutions, which verifies that for this set of parameters, the simplified solution given by Eq. (52) is, indeed, a good approximation to Eq. (33). The largest error occurs for the case with the largest $\Delta T_l'$. It is also clear that J' approaches a constant both when $X \ll X_c$ and when $X \gg 1$.

When $X \ll X_c$, we are in a kinetically-limited regime and the mass flux approaches the maximum constant value given by the pure vapor limit of Eq. (50). When $X \gg X_c$, we are in a diffusion-limited regime, where the mass flux is limited by how fast the evaporating vapor can diffuse through the noncondensable gas. In the diffusion-limited regime, there are two characteristic behaviors. First, when $X_c \ll X \ll 1$, the slope of the curve in Fig. 2a is nearly equal to -1, reflecting the $1/X$ behavior of the mass flux. Second, when $X \gg 1$, the mass flux approaches another constant value given by Eq. (37) as the system becomes saturated with noncondensable gas. All of these limits are captured by Eq. (52). Note that for a fixed value of X, we have the intuitive result that J' increases as $\Delta T_l'$ increases.

The mass flux approaches a constant when $X \gg 1$ because $\omega \to 0$ and the total density approaches a constant, $\rho_m \to \bar{p} m_g / R T_{l0}$ (assuming the small temperature drop approximation). However, ρ_m is still proportional to $\bar{p}$ which increases without bound as $X \to \infty$. As a result, the mass balance condition given by $dJ/dz = 0$ reduces to $d^2\omega/dz^2 = 0$ by making use of Eq. (13), which yields a linear mass fraction profile. The vapor mass fraction is related to the vapor partial pressure through Eq. (10), but since $\bar{p} \gg p_v$ and $p_v \approx p_s$, they reduce to $\omega_0 = m_v p_{s0}/m_g \bar{p}$ and $\omega_d = m_v p_{sd}/m_g \bar{p}$. Thus, $d\omega/dz = -m_v \Delta p_s / m_g \bar{p} d$, and if we substitute all of this into Eq. (13), we find that $J = D_m m_v \Delta p_s / R T_{l0} d = J_{min}$ in this limit, which is exactly the same as $J'_{min} J_{a0}$, with J'_{min} taken from its definition in Eq. (37). Thus, the mass flux approaches a constant value because the mass fraction profile becomes linear when $X \gg 1$.

In Fig. 2b the evaporative mass flux is plotted for three different values of X_c. Physically, for a fixed vapor composition and operating conditions, variations in X_c can be solely brought about by using a different noncondensable gas (different diffusivity D_m) or by moving the interfaces closer or farther apart (changing d). For a fixed mole ratio X, J' increases as D_m increases or d is decreased, in accordance with physical intuition. Note that in all the cases presented here, the mass flux approaches the same constant value as $X \to 0$ since this value represents a kinetic limit that is unaffected by changes in the diffusivity. However, the transition to this constant occurs at a smaller mass fraction as X_c decreases since the transition to this kinetic regime occurs around $X \approx X_c$.

The mass flux J' is plotted as a function of the temperature drop $\Delta T_l'$ for several fixed values of X and X_c in Fig. 2c and d. Note that J' has a nearly linear dependence on the temperature drop and that the error of the simpler approximation provided by Eq. (52) increases slightly as $\Delta T_l'$ increases.

When J' is scaled by its minimum value J'_{min}, all of the curves in Fig. 2a collapse into a single curve as shown in Fig. 3. This shows that most of the temperature dependence is captured by the parameter J'_{min} within this parameter range.

From a practical standpoint, it is unlikely that the evaporative mass flux will ever approach its absolute kinetic limit for most normal circumstances because the heat flux required to sustain such a

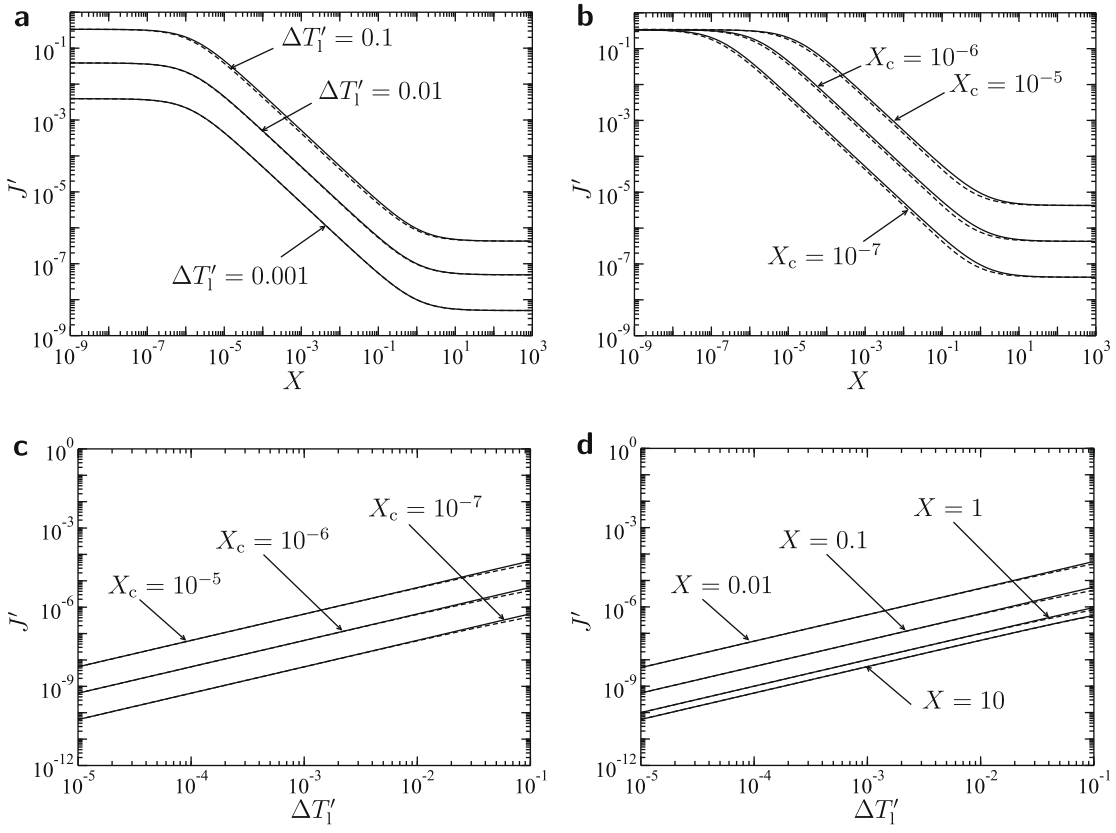

Fig. 2. A plot of the dimensionless mass flux J' as computed from Eq. (33) (solid line) or Eq. (52) (dashed line) when $B = 5$ as a function of (a) X with $X_c = 10^{-6}$, (b) X with $\Delta T_l' = 0.1$, (c) $\Delta T_l'$ with $X = 0.1$, (d) $\Delta T_l'$ with $X_c = 10^{-6}$.

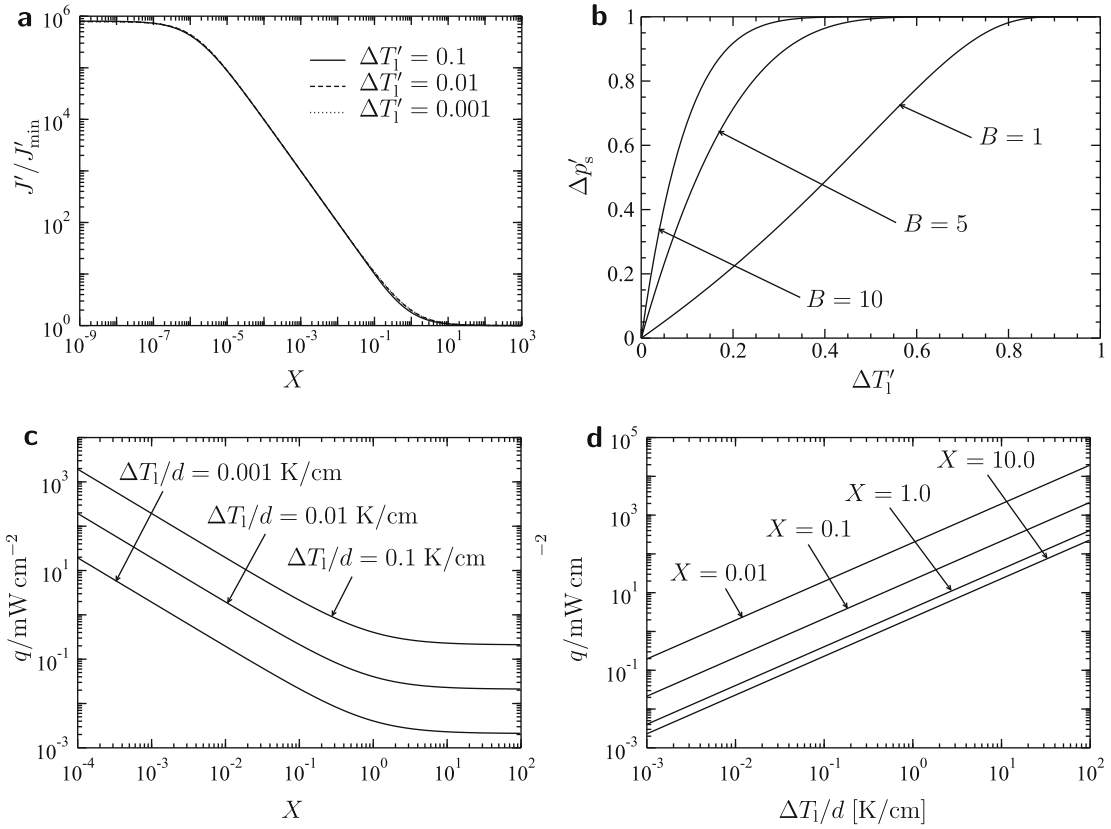

Fig. 3. A plot of (a) the dimensionless mass flux $J'/J'_{\min}$ (scaled by the minimum mass flux) as a function of the relevant dimensionless parameters X and $\Delta T'_l$ with $X_c = 10^{-6}$, (b) the relationship between the dimensionless saturation pressure drop $\Delta p'_s$ and liquid temperature drop $\Delta T'_l$ according to Eq. (40), a plot of the heat flux versus (c) mole ratio X and (d) temperature gradient for a mixture of hydrogen and helium gas.

large mass flux is prohibitively high. To show this explicitly, an energy balance across the liquid and vapor sides of the condensing interface along with the temperature solution provided by Eq. (16) can be used to obtain the following expression for the liquid-side conductive heat flux at that interface,

$$q = q_{ld} = LJ - k_m\left|\frac{dT_v}{dz}\right|_{z=0} + c_{pl}\Delta T_l J = (L + c_{pl}\Delta T_l)J + k_m\frac{\Delta T_v}{d}\frac{Jc_{pv}d/k_m}{\exp(Jc_{pv}d/k_m) - 1}. \quad (54)$$

The last term in Eq. (54) represents the conductive contribution to the vapor heat flux, which has a maximum value of $k_m\Delta T_v/d$ at $Jc_{pv}d/k_m = 0$ and becomes smaller as $Jc_{pv}d/k_m$ increases. If we assume that $c_{pl}\Delta T_l \ll L$ (small temperature drop limit), then a good engineering approximation to Eq. (54) that has the correct limiting behavior as $J \to 0$ and $J \to \infty$ is,

$$q = LJ + k_m\frac{\Delta T_v}{d}. \quad (55)$$

This equation indicates that the major contributors to the heat flux are simply the latent heat of vaporization and conduction through the vapor, which can become large as the interfaces move closer together. If we further assume that differences in the saturation pressures are relatively small, $\Delta p'_s \ll 1$, (which would not be true unless $B\Delta T'_l \ll 1$ as shown in Fig. 3b) and that $|J'| \ll 1$ to ignore the interfacial temperature discontinuity, then we can assume $\Delta T_v = \Delta T_l$ and substitute Eq. (43) for J into Eq. (55), arriving at,

$$q = \left[\kappa\left(1 + \frac{1}{X}\right) + k_m\right]\frac{\Delta T_l}{d}, \quad (56)$$

where κ is a parameter with the units of a thermal conductivity,

$$\kappa = \frac{LX_cBJ_{a0}d}{T_{l0}} = \frac{L^2m_v^2D_mp_{s0}}{R^2T_{l0}^3}. \quad (57)$$

Note that κ depends only on material properties and the operating temperature. For most cases of engineering interest, κ is the most important parameter resulting from this analysis.

It is also possible to define an effective heat transfer coefficient h for this process by writing Eq. (56) as $q = h\Delta T_l$, with h defined by,

$$h = \frac{\kappa}{d}\left(1 + \frac{1}{X}\right) + \frac{k_m}{d}. \quad (58)$$

Note that h decreases as X increases, meaning a smaller heat flux is required to maintain the same temperature drop as the amount of noncondensable gas increases. Another way of stating this is that the resistance to evaporation due to the presence of the noncondensable gas depends both on the amount of gas present (through X) as well as on the ease by which the vapor molecules can diffuse through that gas as measured by the parameter κ (which is proportional to the diffusivity D_m).

In the limit of large quantities of noncondensable gas $(X \to \infty)$, q approaches the constant $q_{\min}$ given by,

$$q_{\min} = LJ_{\min} + k_m\frac{\Delta T_l}{d} = (\kappa + k_m)\frac{\Delta T_l}{d}. \quad (59)$$

This is the minimum heat flux required to sustain the temperature gradient $\Delta T_l/d$ between the interfaces regardless of the amount of the amount of noncondensable gas. In this context, κ can be interpreted as an effective thermal conductivity due to mass transfer since it plays exactly the same role as k_m. Thus, Eq. (56) can also be written as,

$$q = q_{\min} + \frac{\kappa}{X}\frac{\Delta T_l}{d}. \tag{60}$$

The heat flux versus X required to sustain a specified liquid temperature drop, as computed from Eq. (60), is shown in Fig. 3c assuming the noncondensable gas is helium. Note that the heat flux approaches a minimum as X increases. Similar plots are shown in Fig. 3d as a function of the temperature gradient.

Eq. (56) can be solved for the temperature gradient to yield,

$$\frac{\Delta T_l}{d} = \frac{q}{\kappa(1+X^{-1})+k_m}. \tag{61}$$

This equation can be used to predict the expected temperature gradient produced between evaporating and condensing sites for given values of q and X. This is useful for practical problems where the distribution of q near the interface is known from a separate heat-transfer analysis, and one needs an estimate of the expected temperature variation between two interfaces or even between two different evaporating and condensing sites on the same interface separated by a distance d. This is plotted in Fig. 4 for a mixture of hydrogen and helium gas for several values of q.

It is clear that the temperature gradient decreases rapidly by many orders of magnitude as the amount of noncondensable gas is reduced. In the opposite limit as $X \to \infty$, it approaches a constant maximum value as the effective thermal conductivity approaches the constant $k_m + \kappa$. Note, in particular, that when q is small, the temperature gradient remains small no matter how much noncondensable gas is present. In this case, the mass flux is heat-transfer limited because there is insufficient energy for evaporation to proceed. However, when q is larger, the temperature gradient grows rapidly with just a trace amount of noncondensable gas and is not limited by the heat transfer as shown by the curves in Fig. 4b.

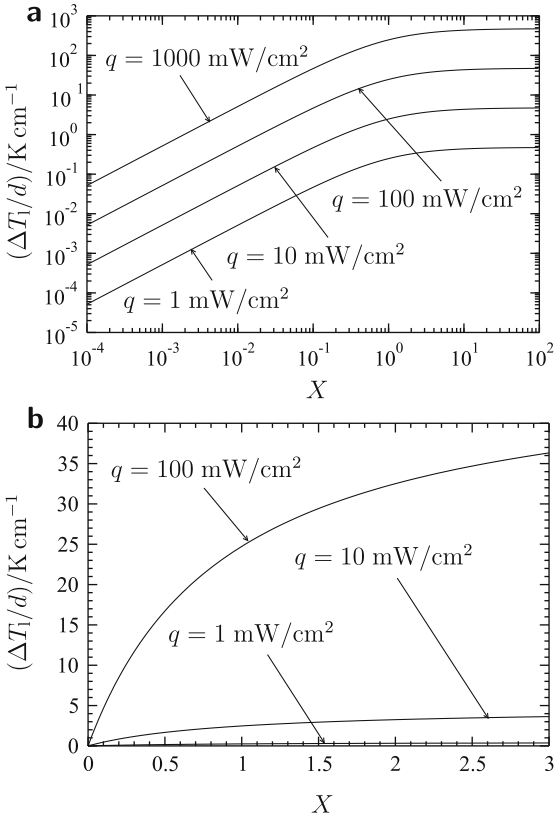

Fig. 4. A plot of the expected temperature gradient versus mole ratio X for a mixture of hydrogen and helium gas for several values of q (a) on a log – log plot, (b) with linear axis scales.

To better understand this behavior, consider the following interpretation. When q is fixed, J is also essentially fixed as apparent from Eq. (55) if the conductive term is neglected. However, J can be decomposed into both convective and diffusive contributions as shown in Section 2.2, with the diffusive term becoming more important as more noncondensable gas is added (decreasing ω). Unlike the diffusive term, the convective term does not give rise to mass fraction gradients. For small amounts of noncondensable gas, J is mostly convective, there is no significant mass fraction gradient, and, hence, there is no significant temperature drop. However, as the amount of noncondensable gas is increased, the diffusive contribution becomes more important and large mass fraction gradients are possible as long as there is sufficient energy being supplied by q for evaporation. A large mass fraction gradient gives rise to a vapor partial pressure gradient which, in turn, leads to a larger interfacial temperature drop. In the limit of large amounts of noncondensable gas ($\omega \to 0$ or $X \gg 1$), the diffusive term dominates as convection becomes negligible and all of the vapor mass flux J is transported by diffusion. Thus, the temperature drop approaches a constant value as $X \gg 1$.

Yet another way of rearranging Eq. (56) is to solve for the required mole ratio X that yields a desired temperature gradient if the interfacial heat flux is known,

$$X = \frac{\kappa}{q(\Delta T_l/d)^{-1} - k_m - \kappa} = \frac{\kappa}{q - q_{\min}}\frac{\Delta T_l}{d}. \tag{62}$$

Obviously, this only makes sense if the denominator is positive, which is just another way of stating the requirement that the temperature gradient can never be greater than $q/(\kappa + k_m)$.

This approach can also provide some insight into the case of a single interface undergoing simultaneous evaporation and condensation at different sites on the interface separated by an average distance d. This estimate of the interfacial temperature gradient can be used along with knowledge of the temperature dependence of the surface tension to assess the likelihood of experiencing Marangoni convection under certain conditions. If the temperature difference between the evaporating and condensing regions is ΔT_l, then the interfacial temperature gradient can be approximated by $\Delta T_l/d$. The heat flux required to sustain this interfacial temperature gradient can be estimated from Eq. (56). Thus, if the heat flux differential is known and the mole ratio of the noncondensable gas is X, then the interfacial temperature gradient can be predicted from Eq. (61). If the heat flux differential and desired temperature interfacial gradient are known, then Eq. (62) can be used to predict the required mole ratio.

In order to demonstrate the application of these equations in a practical engineering situation, we will examine the cryogenic storage of hydrogen in a tank pressurized with helium. The goal is to determine the mole fraction of noncondensable gas (helium) that can produce an interfacial temperature gradient of 1 K/cm, which is potentially large enough to instigate Marangoni (surface-tension driven) convection within the liquid. The subsequent mixing effect could be used to destratify the liquid in the tank without having to rely entirely upon an active mixing strategy using inefficient pumps that are prone to failure.

Consider hydrogen at its normal boiling point. Using the value of D_m computed earlier, we see that $\kappa = 19363$ erg/cm s K for the hydrogen–helium mixture under these conditions, and if we assume the mixture thermal conductivity is equal to that of pure hydrogen vapor ($k_m = k_v = 1714$ erg/cm s K), then a minimum required heat flux of $q_{\min} = 2.11$ mW/cm^2 is predicted from Eq. (59). This is the minimum heat flux required to sustain a temperature gradient of $\Delta T_l/d = 1$ K/cm when there is a large amount of

noncondensable gas present. If the actual interfacial heat flux differential between evaporating and condensing regions were known from a separate thermal analysis to be $q = 100\ \mathrm{mW/cm^2}$ (a value much greater than $q_{\min}$), then the noncondensable mole ratio required to sustain this temperature gradient is about $X = 0.02$ as predicted by Eq. (62). These values can also be obtained by just visually inspecting Fig. 4.

It is instructive to compare the previous situation to the case where there is only pure vapor present. In that case, we can neglect the conductive contribution in Eq. (55) and just assume $q \approx LJ$, and we can also use Eq. (50) for the pure vapor limit to estimate J. For the example just considered, let's assume $T_{l0} = 20.39\ \mathrm{K}$ and $T_{ld} = 19.39\ \mathrm{K}$. The corresponding saturation pressures are $p_{s0} = 1.01325 \times 10^6\ \mathrm{dyn/cm^2}$ and $p_{sd} = 0.77113 \times 10^6\ \mathrm{dyn/cm^2}$ as computed from Eq. (21) using the properties in Table 1. Thus, $\Delta p'_s = 0.24$. We also compute $J_{a0} = 13.93\ \mathrm{g/cm^2\,s}$ from Eq. (20) assuming $\alpha = 1$. Then, from the dimensional form of Eq. (50), we find that $J = J_{a0}\pi\Delta p'_s/4 = 2.63\ \mathrm{g/cm^2\,s}$, from which it follows that $q = LJ = 1.2 \times 10^{10}\ \mathrm{erg/cm^2\,s} = 1200\ \mathrm{W/cm^2}$. This heat flux is about 10,000 times larger than the heat flux predicted for the previous case where there was just 2% noncondensable gas present. These two examples underscore the fact that it is very unlikely to have any significant variation in the interfacial temperature in the absence of a noncondensable gas.

5. Summary

The relationship describing mass flux as represented by Eq. (33) identifies three distinct mass-transport regimes depending on the relative magnitude of the characteristic noncondensable mole ratio X as compared to the critical characteristic mole ratio X_c. When $X \ll X_c$, the system is in a *kinetically-limited* regime where the mass flux approaches an upper limit dictated by kinetic effects. When $X_c \ll X \ll 1$, the kinetic effects become negligible and the mass flux is determined by a combination of diffusive and convective contributions with the diffusive contribution becoming more important as X increases. Finally, when $X \gg 1$, the system is in a *diffusively-limited* regime where the mass flux approaches another constant value as the system becomes saturated with noncondensable gas.

A uniformly-valid approximation of Eq. (33) is also developed by considering various limits of this equation in each regime. The result is an explicit relationship for the mass flux as given by Eq. (52) that is more amenable to efficient and quick engineering analysis in considering various design options. Numerical results indicate that the explicit approximation agrees very closely with the implicit relationship over the entire range of X. It is expected that for most engineering applications of interest in the field of cryogenic fluid storage, the explicit relationship will yield satisfactory predictions. In particular, this equation is used to derive useful relationships between the mole ratio, temperature difference and the required heat flux as long as the mass flux is not in a kinetically-limited regime. For most practical circumstances, the evaporative mass flux will be many orders of magnitude less than its kinetic limit, so this relationship is valid for many situations of interest.

Perhaps the most important practical consequence of this paper is the prediction of an effective heat transfer coefficient between the evaporating and condensing interfaces that relates the heat flux to the temperature drop across the vapor gap, including contributions from both heat and mass transfer, as expressed by Eq. (58).

6. Conclusions

In this paper, a one-dimensional model of heat and mass transport across a binary gas mixture between two planar evaporating and condensing interfaces held at different temperatures is developed in order to examine the leading-order effects of a noncondensable gas. This analysis accounts for vapor diffusion through the noncondensable gas as well as the nonequilibrium interfacial boundary conditions that become important if the rate of evaporation approaches its kinetic limit. By balancing the mass and energy fluxes between these interfaces, the problem is reduced to solving two implicitly-coupled, integro-algebraic equations given by Eqs. (22) and (23) for the two unknowns J and $\bar{p}$. Invoking a reasonable assumption that the temperature drop between the two interfaces is relatively small, the system of equations is reduced to a single implicit relationship for the mass flux given by Eq. (33).

Application of the relationships developed as part of this analysis to a particular situation involving the cryogenic storage of liquid hydrogen has led to two important conclusions:

(1) In the absence of a noncondensable gas, the interfacial temperature is uniform and equal to the saturation temperature. In this case, an enormous heat flux is required to produce any appreciable nonuniformity in the interfacial temperature.
(2) In the presence of even a minute amount of noncondensable gas, temperature variations can be sustained between different evaporating and condensing sites on the vapor–liquid interface at quite moderate heat fluxes. In this situation, surface-tension variations caused by the resulting interfacial temperature gradients could potentially give rise to Marangoni convection that could be exploited to destratify the liquid.

The most important effects of the noncondensable gas are described by a single parameter κ defined by Eq. (57). This parameter only depends on the noncondensable gas through the mass diffusion coefficient. Because of its relative simplicity, Eq. (56) can be manipulated in a variety of ways to be able to explicitly solve for any variable of interest in terms of the other variables. In particular, the expected temperature variations generated along an interface can be predicted using Eq. (61) if the surrounding thermal field (heat fluxes) and noncondensable mole ratio are known.

Future improvements to this model that are currently in progress entail the incorporation of a more comprehensive kinetic treatment of an evaporating interface, including the effects of the noncondensable gas on the kinetics, which were not considered in this work. In addition, a more rigorous analysis of the properties of a multi-component mixture will also be incorporated to account for departures from ideal gas behavior. It is understood that this simple one-dimensional model has inherent limitations for predicting the precise quantitative behavior of real systems since complex geometries, boundary conditions, and thermophysical properties of the fluids and of the container walls and/or other structures will inevitably come into play. Nevertheless, it is hoped that this simple model will provide valuable quantitative insight into the basic mechanisms at play and allow order of magnitude estimates to be performed for quick engineering analysis and judgment.

Acknowledgement

This work has been supported by the Cryogenic Fluid Management (CFM) Project at NASA Glenn Research Center through funds provided by the Exploration Systems Divisions at NASA Headquarters.

References

[1] J.A. Clark, Review of pressurization, stratification, and interfacial phenomena, Adv. Cryogen. Eng. 33 (10) (1965) 259–283.

[2] W.J. Minkowycz, E.M. Sparrow, Condensation heat transfer in the presence of noncondensables, interfacial, resistance, superheating, variable properties and diffusion, Int. J. Heat Mass Transfer 9 (1966) 1125–1144.
[3] R.W. Schrage, A Theoretical Study of Interphase Mass Transfer, Columbia University Press, New York, 1953.
[4] D.A. Labuntsov, A.P. Kryukov, Analysis of intensive evaporation and condensation, Int. J. Heat Mass Transfer 22 (7) (1979) 989–1002.
[5] L. Pong, G.A. Moses, Vapor condensation in the presence of a noncondensable gas, Phys. Fluids 29 (6) (1986) 1796–1804.
[6] K. Aoki, S. Takata, S. Kosuge, Vapor flows caused by evaporation and condensation on two parallel plane surfaces: effect of the presence of a noncondensable gas, Phys. Fluids 10 (6) (1998) 1519–1533.
[7] K. Aoki, S. Takata, S. Taguchi, Vapor flows with evaporation and condensation in the continuum limit: effect of a trace of noncondensable gas, Eur. J. Mech. B/Fluids 22 (1) (2003) 51–71.
[8] K. Aoki, S. Takata, S. Taguchi, Vapor flows with evaporation and condensation in the continuum limit: effect of a trace of noncondensable gas, Eur. J. Mech. B/Fluids 22 (1) (2003) 51–71.
[9] D. Bedeaux, Nonequilibrium thermodynamics and statistical physics of surfaces, Adv. Chem. Phys. 64 (1986) 47–109.
[10] D. Bedeaux, L.J.F. Hermans, T. Ytrehus, Film boiling heat transfer from a horizontal surface, Physica A 169 (1990) 263–280.
[11] D. Bedeaux, S. Kjelstrup, Transfer coefficients for evaporation, Physica A 169 (1999) 413–426.
[12] J.W. Cipolla, H. Lang, S.K. Loyalka, Kinetic theory of condensation and evaporation. II, J. Chem. Phys. 61 (1) (1974) 69–77.
[13] Y. Sone, Y. Onishi, Kinetic theory of evaporation and condensation, J. Phys. Soc. Japan 35 (1973) 1773–1776.
[14] J. Ge, D. Bedeaux, J.M. Simon, S. Kjelstrup, Integral relations, a simplified method to find interfacial resistivities for heat and mass transfer, Physica A 385 (2007) 421–432.
[15] M.Bond, Non-equilibrium evaporation and condensation, Ph.D. thesis, Univeristy of Victoria, 2000..
[16] M. Bond, H. Struchtrup, Mean evaporation and condensation coefficients based on energy dependent condensation probability, Phys. Rev. E 70 (2004) 061605–061625.
[17] G. Fang, C.A. Ward, Temperature measured close to the interface of an evaporating liquid, Phys. Rev. E 59 (1) (1999) 417–428.
[18] G. Fang, C.A. Ward, Examination of the statistical rate theory expression for liquid evaporation rates, Phys. Rev. E 59 (1) (1999) 441–453.
[19] C.A. Ward, D. Stanga, Interfacial conditions during evaporation or condensation of water, Phys. Rev. E 64 (1) (2001). 051509–051509–9.
[20] C.A. Ward, G. Fang, Expression for predicting liquid evaporation flux: statistical rate theory approach, Phys. Rev. E 59 (1) (1999) 429–440.
[21] M.S. Plesset, Note on the flow of vapor between liquid surfaces, J. Chem. Phys. 20 (5) (1952) 790–793.
[22] R.B. Bird, W.E. Stewart, E.N. Lightfoot, Transport Phenomena, second ed., John Wiley and Sons Inc., New York, 2002.
[23] J.O. Hirschfelder, C.F. Curtiss, R.B. Bird, Molecular Theory of Gases and Liquids, Wiley, New York, 1964. p. 584.
[24] C.H. Panzarella, Nonlinear analysis of horizontal film boiling, Ph.D. thesis, Northwestern University, Evanston, IL, 1998..
[25] E.W. Lemmon, M.O. McLinden, D.G. Friend, Thermophysical properties of fluid systems, in: P. Linstrom, W. Mallard (Eds.), NIST Chemistry WebBook, NIST Standard Reference Database Number 69, National Institute of Standards and Technology, Gaithersburg MD, 20899, 2005..